Indian Journal of Pure & Applied Physics
Vol. 58, September 2020, pp. 673-677

Quantitative analysis of Fe/Co co-doped ZnO by Rietveld method

Bidyarani Maibam[a], Saptaka Baruah[a], Beer Pal Singh[b] & Sanjeev Kumar[a*]

[a]Center of Advance Studies, Department of Physics, Rajiv Gandhi University, Doimukh, Itanagar, India

[b]Department of Physics, CCS University, Meerut, India

Received 23 December 2019; accepted 4 March 2020

Fe/Co co-doped Zinc oxide was prepared by using hydrothermal method. Refinement of recorded X-ray diffractograms was done by *Rietveld* method by using MAUD. It shows that all the samples have a hexagonal structure with space group P63mc and the average crystallite size of the samples lie between 49-79 nanometers. Presence of some secondary phases were also detected. *Rietveld* analysis data reveals that the density of the doped and co-doped ZnO is more than the pristine ZnO. The goodness of fit value ranges from 1.3875-1.7519. The unit cell volume decreases for the doped and co-doped ZnO as the value of lattice parameter decreases with doping and co-doping. Decrease in the interplaner spacing values may be because of the strain developed in the lattice due to doping and co-doping.

Introduction

ZnO is a compound semiconductor of II-VI group, and its ionicity lies in the boundary between the ionic and covalent semiconductor[1,2]. ZnO has attracted much attention for its potential application in electronics, optoelectronics and laser technology because of its high exciton binding energy (60 meV), large bandgap energy (3.37 eV), high thermal and mechanical stability at room temperature and exceptional electrochemical properties due to its large surface to volume ratio[1,3]. Of the two main crystallize form of ZnO *i.e.* hexagonal and zinc blend structure, the most common and stable at ambient conditions is wurtzite structure(hexagonal) belonging to P63mc space group[4]. It is characterized by two interconnecting sub lattices of Zn^{2+} and O^{2-} in such a way that each O^{2-} ion is surrounded by tetrahedral of Zn^{2+} ions and vice versa. ZnO can also be used as sensor, converter, and energy generator in hydrogen because of its strong piezoelectric and pyro-electric properties. The piezoelectric and pyroelectric properties arise due to the large electrochemical coupling together with lack of symmetry in wurtzite[5].

Rietveld method has been effectively used for the study of data acquired from different experimental techniques. It is one of the most important means for the analysis of structural and microstructural properties of various crystalline materials. .The large degree of success of the *Rietveld* method is because of its ability to analyse the complex diffraction patterns of Bragg peaks with severe overlapping[1]. It is well established that the *Rietveld* refinement method has many advantages over the traditional method where the selected individual reflection is used for estimating the weight fraction. *Rietveld* method takes into account all the reflections for each phase leading to the minimization of overlapped peaks problem[7]. *Rietveld* method gives a more precise estimation of relative phase proportion as it can consider the texture effect during fitting while the techniques using integrated intensities of individual peaks suffer severe drawback in obtaining the consistent results in the quantitative analysis due to the presence of preferred orientation effect[8]. Adding to the above advantages, the information required in *Rietveld* method for the quantitative analysis is small and is associated with the phases of crystal structure eliminating the requirement of a standard[6].

In this work pristine, doped and co-doped samples were prepared by hydrothermal method. The structural analysis was done by *Rietveld* analysis method.

Experimental process

Pristine, doped and co-doped samples were prepared by using Zinc nitrate Hexahydrate ($Zn(NO_3)2.6H_2O$), Sodium Hydroxide (NaOH), Ferric Nitrate Nonahydrate ($Fe(NO_3)_3.9H_2O$), Cobaltous Nitrate Hexahydrate ($Co(NO_3)_2.6H_2O$)as precursor materials. The samples were prepared using hydrothermal technique.

The X-ray diffraction profile of the pristine, doped and co-doped sample is recorded. The XRD

* Corresponding author: Email: sanjeev.kumar@rgu.ac.in

measurements were done at the operating voltage of 40KV and tube current of 15mA. The step scan data of step size 0.002° 2θ and scan speed of 5-10° per sec depending on the intensity of various peaks with the angular range of 5° to 90° of the experimental peaks were recorded.

Structural analysis

Fig. 1(a) shows XRD pattern of $Zn_{1-x-y}Fe_xCo_yO$. The shift of peaks towards the higher angle side for the (001), (002) and (101) planes in the XRD pattern compare to that of the pristine ZnO are clearly visible in Fig. 1(b). This may be because of the substitution of dopants of slightly different ionic radii (Co^{2+}=0.58Å, Fe^{2+}=0.63Å, Fe^{3+}=0.49Å) than that of the host cation (Zn^{2+}=0.60Å)[2,3].Considerable decrease in intensity of the X-ray diffraction peaks of the doped and Fe/Co co-doped ZnO compare to that of the pure ZnO also indicates that the crystalline character of ZnO had decreased significantly with Fe and Co doping. A considerable decrease in the crystallinity of ZnO with doping indicates the presence of lattice defects such as oxygen vacancy and Zinc interstitial[11]. It is important to note that addition of Co as the co-dopant into the Fe doped ZnO reduces the crystalline quality significantly. So, the observed decrease in crystallinity may be attributed to the increase in the density of crystal defects caused by co-doping. The crystallite size is calculated by using *Scherrer's* formula[12]

$$D = \frac{0.9\lambda}{\beta cos\theta}$$

Where, $\lambda = 0.154$ nm, wavelength of the incident X-ray, θ is the Bragg's diffraction angle and β is the full width half maximum (FWHM) value corresponding to (101) plane which has the highest intensity. Fig. 2 shows the variation of crystallite size and FWHM with different doping concentrations of Fe and Co ions**.** The crystallite size calculated by using *Scherrer's* equation is in accordance with the full width half maximum value as tabulated in Table 1.

In this study, *Rietveld's* powder structure refinement method was used to find the refine

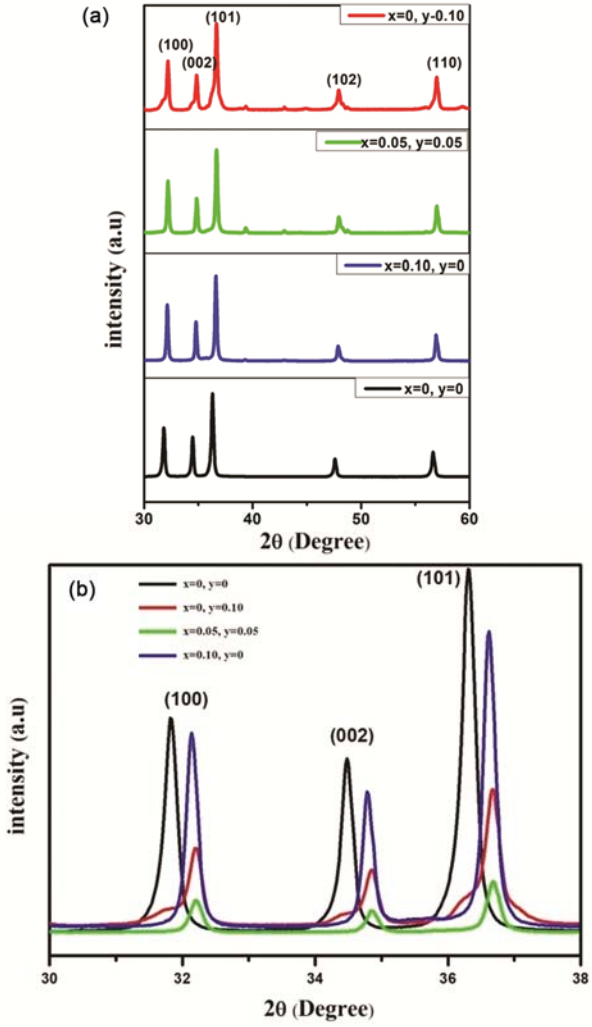

Fig. 1 — (a) XRD pattern of $Zn_{1-x-y}Fe_xCo_yO$ (x=0, 0.05, 0.10, y=0, 0.05. 0.10) (b) XRD pattern of first three peaks of $Zn_{1-x-y}Fe_xCo_yO$

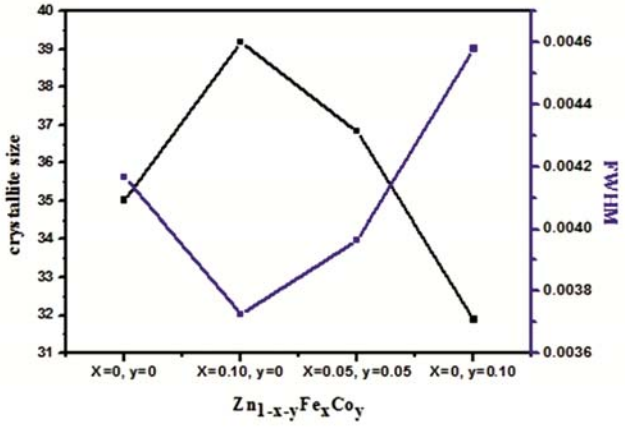

Fig. 2 — FWHM and crystallite size for $Zn_{1-x-y}Fe_xCo_yO$ (x=0, 0.05, 0.10, y=0, 0.05. 0.10)

Table 1 — crystallite size calculated from Scherrer's formula

Zn1-x-yFexCoyO	Crystallite size (nm) (Scherrer's)
X=0, y=0	35.0164
X=0.10, y=0	39.1771
X=0.05, y=0.05	36.839
X=0, y=0.10	31.8856

structural parameters such as lattice parameters, density, *etc.* and microstructural parameters such as particle size and rms strain *etc*. Pseudo Voigt analytical function which takes into account of both the particle size and strain broadening of the experimental profile was adopted for fitting[3]. The *Rietveld* analysis of powder diffraction data was done by using MAUD (material analysis using diffraction) program, version 2.91. In Maud, the effect of crystal size distribution is taken on the variance of two peak shape functions namely Lorentzian and Gaussian.

Minimization of observed and simulated powder diffraction patterns difference was done by Marquardt least squares method, considering that the integrated intensity of the peak is a function of structural parameters only[13]. The refinement quality is given by some reliability indexes like weight profile GoF, $R_{wp,}$ $R_{exp,}$ R_b[14]. R_{wp} is the most important R factor as the quantity that is actually minimized in the least squares is the numerator of R_{wp}[15]. The refinement process is said to be successful if R_{wp} is decreasing. GoF value should be low and approaches to 1. It represents the standard setting for experimental XRD patterns result. R_{exp} and R_b are expected weighted profile factor and the Bragg factor, respectively.

They are defined by the following relations:

$$GoF = \frac{R_{wp}}{R_{exp}}$$

$$R_{wp} = \left[\frac{\sum w_i (I_{io} - I_{ic})^2}{w_i I_{io}^2}\right]^{\frac{1}{2}}$$

$$R_b = \frac{\sum (I_{ko} - I_{kc})}{\sum I_{ko}}$$

$$R_{exp} = \frac{N - P}{\sum w_i I_{io}^2}$$

Where, I_{io} is the observed intensities at the i^{th} step, I_{ic} is the calculated intensities at the i^{th} step. I_k signifies the intensities of the k^{th} Bragg reflection at the completion of refinement.$w_i = \frac{1}{I_{io}}$ gives the weight factor. $(N - P)$ represent the number of degrees of freedom.

The *Rietveld* analysis of the XRD pattern shows the formation of a hexagonal wurtzite structure as the peaks correspond to the plane of the hexagonal wurtzite structure. The theoretical and observed patterns are fitted quite successfully, as shown in Fig. 3. The pattern also indicates the presence of some impurity phase & such as Co_3O_4, Fe_2O_3, etc. in the doped and co-doped sample.

Fig. 4 shows comparison of crystallite size calculated from *Scherrer's* formula and obtained from *Rietveld's* analysis. The difference in crystallite size obtained from Rietveld analysis and as calculated by using *Scherrer's* formula may be attributed to the

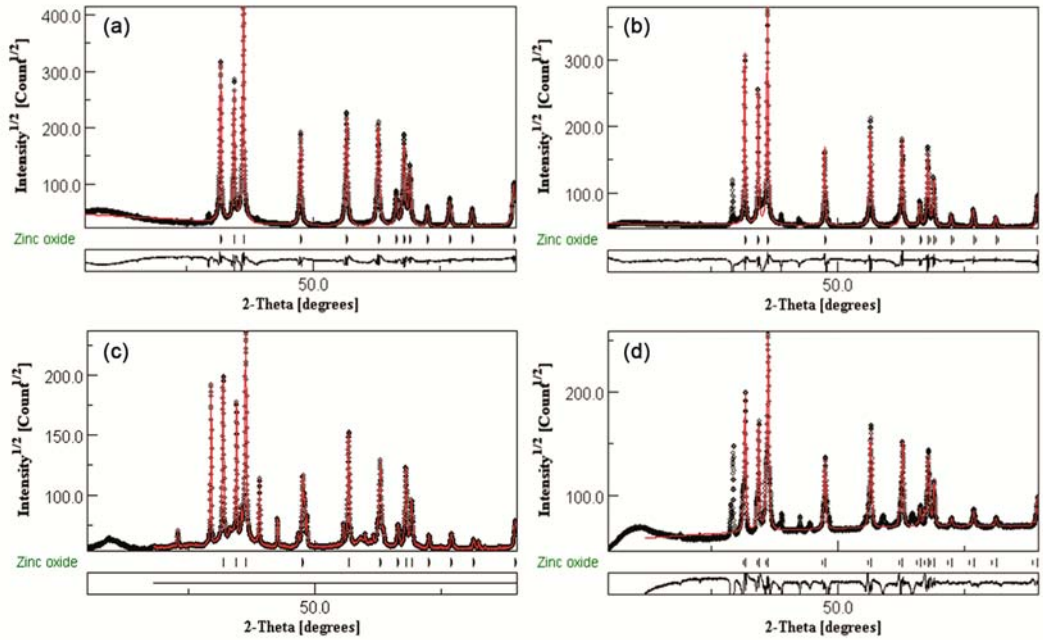

Fig. 3 — Rietveld's analysis output pattern of $Zn_{1-x-y}Fe_xCo_yO$ (a) x=0, y=0 (b) x=0.10, y=0 (c) x=0.05, y=0.05 (d) x=0, y=0.10

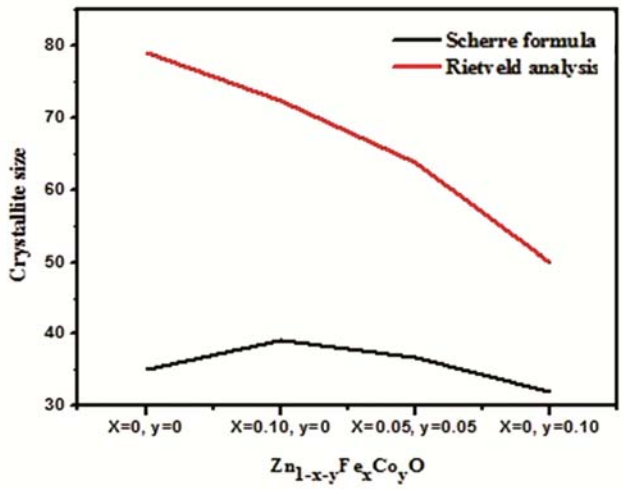

Fig. 4 — Comparison of crystallite size calculated from Scherrer's formula and obtained from Rietveld's analysis

development of lattice strain in the samples. *Rietveld* analysis takes account of lattice strain whereas *Scherrer's* formula excluded the contribution of lattice strain. Therefore, the difference of diffraction peak broadening of different samples not only account for nano-crystallite size but also for the strain and instrumental broadening[16].

The inter-planar spacing was calculated by using[17]

$$\frac{1}{d^2} = \frac{4}{3}\left(\frac{h^2 + hk + k^2}{a^2}\right) + \frac{l^2}{c^2}$$

Hexagonal close packed unit cell volume was calculated by using the relation[4]

$$V = \frac{\sqrt{3}}{2}a^2c = 0.866a^2c$$

The distortion degree was calculated by using the formula, $R = \sqrt{\frac{8}{3}}\frac{a}{c}$.The degree of distortion for ideal wurtzite structure is R=1, as $\frac{c}{a}$ ratio is $\sqrt{\frac{8}{3}}$ .The ratio between the nearest neighbour distance (anion-cation length) and lattice parameter c is given by

The internal parameter, $u = \frac{a^2}{3c^2} + \frac{1}{4}$

Bond length and bond angle were calculated with the help of following formula[17, 19]

$$b = uc$$

$$b_1 = \sqrt{\frac{1}{3}a^2 + \left(\frac{1}{2} - u\right)^2 c^2}$$

$$\alpha = \frac{\pi}{2} + \arccos\left[\left(\sqrt{1 + 3\left(\frac{c}{a}\right)^2\left(-u + \frac{1}{2}\right)^2}\right)^{-1}\right]$$

$$\beta = 2\arcsin\left[\left(\sqrt{\frac{4}{3} + 4\left(\frac{c}{a}\right)^2\left(-u + \frac{1}{2}\right)^2}\right)^{-1}\right]$$

Where, b and b_1 represent the nearest neighbour bond length along c-direction and c-axis bond length between anion and cation atoms respectively. α gives the average basal bond angle $(O_a - Zn - O_b)$ and β the average base apex angle $(O_b - Zn - O_b)$.Where O_a and O_b represents oxygen atom at the apex and at the base of tetrahedral structure respectively.

The structural parameters like lattice constant, particle size, density, *etc*. extracted from the analysis with calculated d value are tabulated in Table 2 and calculated values of c/a ratio, unit cell volume, *etc*. are tabulated in Table 3. The lattice parameters a and c slightly decreases with doping and co-doping, indicating the incorporation of Fe and Co ion in the ZnO matrix. The unit cell volume decreases with doping and co-doping because of the decrease in lattice parameters. It is also observed from the refinement that the crystallite size decreases for doped and co-doped samples. The decrease in crystallite size and lattice parameters is because of the smaller ionic

Table 2 — Value extracted from Rietveld analysis

Zn1-x-yFexCoyO	a=b (Å)	c(Å)	Density	Rwp (%)	Rp	Goodness of fit (GOF) (%)	Crystallite size (nm)	d	Microstrain
x=0, y=0	3.2541	5.2134	5.6537	13.6370	0.10230198	1.7519	79.0446	2.4791	9.804751×10^{-6}
x=0.10, y=0	3.2349	5.1827	5.7560	11.2354	0.07055763	1.5409	72.3646	2.4645	0.0010198378
x=0.05, y=0.05	3.2428	5.1969	5.7184	17.5634	0.09559069	1.6272	63.8647	2.4706	8.631681×10^{-4}
x=0, y=0.10	3.2386	5.1881	5.7256	12.946	0.08676648	1.3875	49.8352	2.4672	0.0013357651

Table 3 — Calculated values of u, R, b, b_1, α, β, c/a, V

Zn1-x-yFexCoyO	u	R	b	b_1	α	β	c/a	V
x=0, y=0	0.3799	1.0192	1.9804	1.9804	108.4364	110.486	1.6021	47.8091
x=0.10, y=0	0.3799	1.0193	1.9687	1.9687	108.4358	110.4865	1.6020	46.9696
x=0.05, y=0.05	0.3798	1.0189	1.9737	1.9737	108.4538	110.4692	1.6026	47.3268
x=0, y=0.10	0.3799	1.0193	1.9709	1.9709	108.4311	110.491	1.6019	47.1247

radius of Fe and Co leading to lattice contraction. The d values of doped and co-doped samples decreases as compared to that of pristine ZnO. This decrease of d value of (101) may be ascribed to the change in bond length and bond angles. The change in the inter-planar spacing may also be because of the strain produced in the lattice[20]. The obtained data also reveals that c/a, u and R Values remain almost constant for all the samples. A significant change in distortion degree R is not expected if the doped ions take the oxidation state Co^{2+} or Fe^{2+} since the difference in ionic radii with the host Zn^{2+} is negligible.

Conclusions

Pristine, doped, and co-doped ZnO nanoparticles were synthesized via hydrothermal technique**.** *Rietveld* analysis of the prepared samples was done by using MAUD software**.** The Difference in theoretically calculated crystallite size and the crystallite size calculated from *Scherrer's* formula was observed. This work gives an accurate quantitative analysis and determines the crystallite size of ZnO.

References

1 Agnieszka K R & Teofil J, *Mater*, 7 *(*2014) 2833.

2 Ozgur U, Alivov Y I , Liu C, Teke A, Reshchikov M A, Dogan S, Avrutin V & Cho S J & Morkoc H, *J Appl Phys*, 98 (2005) 041301.

3 Kundu S, Sain S, Satpati B, Bhattacharyya S R & Pradhan S K, *RSC Adv*, 5 (2015) 23101.

4 Santos D A A, Rocha A D P & Macedo M A, *Powder Diffraction Suppl*, 23 (2008) S36.

5 Parihar V, Raja M & Paulose R, *Rev Adv Mater Sci*, 53 (2018) 119.

6 Albinatiand A & Willis B T M, *J Appl Cryst*, 15 (1982) 361.

7 Ortiz A L , Cumbrera F L, Sanchez-Bajo F, Guiberteau F & Caruso R, *J Eur Ceram Soc*, 20 (2000) 1845.

8 Dollase W A, *J Appl Cryst*, 19 (1986) 267.

9 Singh R P P, Hudiara I S, Panday S & Rana S B, *J Supercond Nov Magn*, 29 (3) (2016) 819.

10 Beltran J J, Barrero C A & Punnoose A, *J Phys Chem C*, 118 (2014) 13203.

11 Park J H, Lee Y J, Bae J S, Kim B S, Cho Y C, Moriyoshi C, Kuroiwa Y, Lee S & Jeong S Y, *Nanoscale Res Lett*, 10 (2015) 186.

12 Mitra A, Mahapatra A S, Mallick A & Chakrabarti P K, *J Magn Magn Mater*, 424 (2017) 388.

13 Bid S & Pradhan S K, *Mater Chem Phys*, 82 (2003) 27.

14 Bhakta N, Inamori T, Shirakami R, Tanioku Y, Yoshimura K & Chakrabarti P K, *Mater Res Bull*, 104 (2018) 6.

15 Izumi F, *Anal Spectros Lib*, 7(1996) 405.

16 Bandyopadhyay A, Modak S, Acharya S, Deb A K & Chakrabarti P K, *Solid State Sci*, 12 (2010) 448.

17 Guruvammal D, Selvaraj S, Sundar S M, *J Magn Magn Mater*, 452 (2018) 335.

18 Sharma D & Jha R, *Ceram Int*, 43 (2017) 8488.

19 Brehm J U, Winterer M & Hahn H, *J Appl Phys*, 100 (2006) 064311.

20 Zak A K, Majid W H A, Abrishami M E & Yousef R, *Solid State Sci*, 13 (2011) 251.